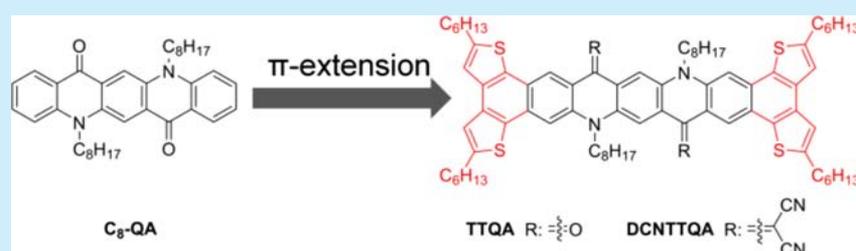


Large  $\pi$ -Conjugated Quinacridone Derivatives: Syntheses, Characterizations, Emission, and Charge Transport PropertiesWeiping Chen,<sup>†</sup> Kui Tian,<sup>‡</sup> Xiaoxian Song,<sup>†</sup> Zuolun Zhang,<sup>\*,†</sup> Kaiqi Ye,<sup>†</sup> Gui Yu,<sup>\*,‡</sup> and Yue Wang<sup>\*,†</sup><sup>†</sup>State Key Laboratory of Supramolecular Structure and Materials, College of Chemistry, Jilin University, Changchun 130012, China<sup>‡</sup>Beijing National Laboratory of Molecular Sciences, Institute of Chemistry, Chinese Academy of Sciences, Beijing 100190, China

## Supporting Information



**ABSTRACT:** Two 11-ring-fused quinacridone derivatives, TTQA and DCNTTQA, have been synthesized by ferric chloride mediated cyclization and Knoevenagel reaction. Replacement of the carbonyl groups (in TTQA) with dicyanoethylene groups (in DCNTTQA) not only red-shifted the emission to the near-infrared region but also led to a nonplanar skeleton that significantly improved the solubility of DCNTTQA. Moreover, dicyanoethylene groups rendered DCNTTQA low-lying HOMO and LUMO levels. DCNTTQA-based solution-processed field-effect transistors showed a hole mobility up to  $0.217 \text{ cm}^2 \text{ V}^{-1} \text{ s}^{-1}$ .

Organic compounds with a large  $\pi$ -extended skeleton have attracted enormous attention as active materials in various electronic devices, such as organic lighting-emitting diodes,<sup>1</sup> organic solar cells,<sup>2</sup> and organic field-effect transistors (OFETs).<sup>3</sup> In addition, they provide a deeper understanding of aromaticity and stability of large  $\pi$ -systems.<sup>4</sup> Among these types of compounds, heterocyclic polycyclic aromatic hydrocarbons (hetero-PAHs) are especially attractive because they possess fascinating features such as structural diversity, high stability, low-energy absorption, and high charge carrier mobility.<sup>5–10</sup> Therefore, there has been increased interest in their design, synthesis, and applications. To construct hetero-PAHs with desirable optoelectronic functions, one method is to extend the  $\pi$ -skeleton of known molecules. Based on this, we propose the molecular design strategy as follows: (i) the parent molecules should have remarkable optical and electronic functions and can be easily modified at multiple active sites; (ii) the aromatic ring fusion and other  $\pi$ -moiety modifications should be able not only to extend the  $\pi$ -conjugation but also to efficiently regulate electronic structures and thus tune the optical and electronic properties; and (iii) the introduced functional and auxiliary groups should afford sufficient solubility for solution processing of the target molecules.

In line with this design strategy, we have carried out studies on hetero-PAHs based on quinacridone (QA in Figure 1). QA derivatives are widely used as industrial pigments<sup>11</sup> and as building blocks for preparing other functional molecules. To date, the supramolecular assembly,<sup>12</sup> polymorphism,<sup>13</sup> as well as photoluminescent,<sup>14</sup> electroluminescent,<sup>15</sup> and photovoltaic properties<sup>16</sup> of many QA derivatives have been investigated.

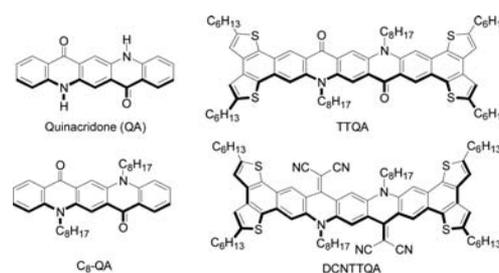


**Figure 1.** Chemical structures of TTQA, DCNTTQA, and the parent molecules (QA and C<sub>8</sub>-QA).

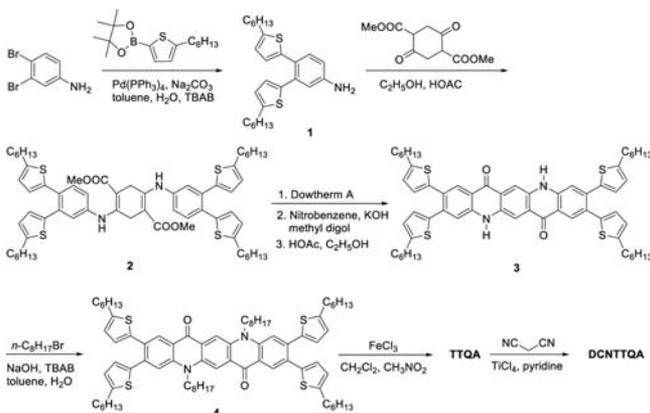
The linear five-ring-fused rigid structure of the QA core endows these compounds with various interesting properties such as bright emission, broad absorption, and strong  $\pi$ - $\pi$  interactions. Furthermore, QAs have remarkable air and thermal stability, and their molecular structures can be easily modified. We have now synthesized QA-based hetero-PAHs TTQA by fusing thiophene rings to the skeleton of a parent C<sub>8</sub>-QA molecule<sup>13b</sup> and DCNTTQA by replacing the carbonyl groups of TTQA with dicyanoethylene (DCN) groups (Figure 1). The electron-rich character of thiophene groups and strongly electron-withdrawing nature of DCN moieties<sup>16b</sup> are expected to strongly influence the electronic structures and various properties of the compounds. Alkyl chains (*n*-hexyl and *n*-octyl) are introduced to the compounds to improve solubility.

Received: November 1, 2015

Published: November 25, 2015

The synthetic routes for TTQA and DCNTTQA are shown in Scheme 1. The condensation reaction of 3,4-bis(5-hexyl-2-

### Scheme 1. Synthetic Procedures of TTQA and DCNTTQA



thienyl)aniline (**1**) and dimethyl succinyl succinate successfully afforded amine derivative **2**, which was then transformed to QA derivative **3** by the annulation reaction in Dowtherm A and the following oxidation of the central cyclohexadiene ring with nitrobenzene.<sup>15</sup> N-Alkylation of **3** provided the key precursor **4**. The oxidative cyclization of **4** in the presence of 10 equiv of ferric chloride afforded TTQA in nearly quantitative yield. With six long alkyl chains, TTQA is poorly soluble in  $\text{CH}_2\text{Cl}_2$  (<0.5 mg/mL), leading to its rapid precipitation from the reaction mixture. The poor solubility might eliminate side reactions such as chlorination of TTQA,<sup>17</sup> thus ensuring the high-yield cyclization. The Knoevenagel reaction of TTQA and malononitrile was performed in pyridine to produce DCNTTQA (>90% yield), which was found to be more soluble in common solvents (>10 mg/mL in  $\text{CH}_2\text{Cl}_2$ ). TTQA and DCNTTQA possess remarkable thermal stability with decomposition temperatures (corresponding to 5% weight loss) of 425 and 378 °C (Figure S1), respectively.

To gain insight into the geometrical and electronic structures of TTQA and DCNTTQA, DFT calculations were performed at the B3LYP/6-31G\* level (Figure 2a). The optimized conjugated skeleton of TTQA is nearly planar, similar to the case of *N,N'*-

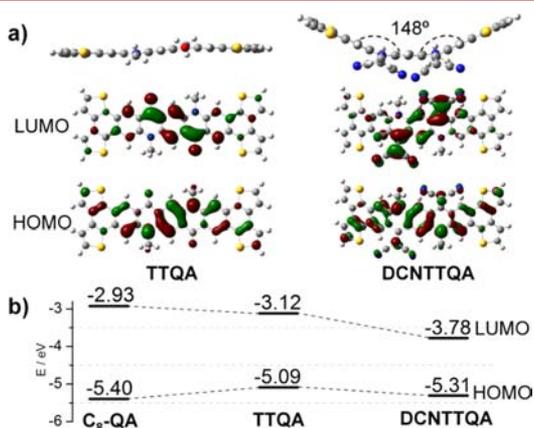


**Figure 2.** (a) DFT-calculated molecular conformations and frontier orbital distributions of TTQA and DCNTTQA (the hexyl and octyl groups are replaced by hydrogen atoms and methyl groups, respectively, for simplification). (b) HOMO and LUMO energy levels of  $\text{C}_8\text{-QA}$ , TTQA, and DCNTTQA obtained from the electrochemical data.

bis(alkyl)-substituted QA.<sup>13a</sup> However, the backbone of DCNTTQA is twisted, showing a “V”-shaped conformation, wherein the two dithienonaphthalene moieties and the two DCN groups bend to the upper and lower sides of the central benzene ring, respectively. The twisted structure is caused by the steric hindrance between the DCN groups and neighboring hydrogen atoms.<sup>18</sup> TTQA with a large planar structure should have a strong aggregation tendency caused by the strong intermolecular  $\pi\text{-}\pi$  interactions, which explains its poor solubility. In contrast, the twisted structure of DCNTTQA can weaken the  $\pi\text{-}\pi$  interactions and make the compound more soluble. Both the HOMO and LUMO of TTQA are mainly distributed on the parent QA skeleton. Although DCNTTQA has a similar HOMO distribution, its LUMO is distributed quite differently, being localized on the DCN groups and the central benzene ring, due to the strong electron-withdrawing ability of DCN groups.

In cyclic voltammetry measurements, both compounds exhibit two sequential quasi-reversible oxidation waves and one quasi-reversible reduction wave (Figure S2). Based on the onset oxidation/reduction potentials (Table S1), the HOMO/LUMO energy levels are calculated to be  $-5.09$  eV/ $-3.12$  eV for TTQA and  $-5.31$  eV/ $-3.78$  eV for DCNTTQA. Therefore, from TTQA to DCNTTQA, replacement of the carbonyl moieties with strongly electron-withdrawing DCN groups significantly lowers the HOMO and LUMO energy levels (Figure 2b). Moreover, the LUMO is more effectively decreased, resulting in an energy gap ( $E_g$ ) for DCNTTQA (1.53 eV) that is much narrower than that of TTQA ( $E_g = 1.97$  eV). Comparison between the energy levels of TTQA and  $\text{C}_8\text{-QA}$  indicates that the fusion of thiophene rings elevates the HOMO level and lowers the LUMO level, leading to a narrower  $E_g$  (Figure 2b and Table S1).

In  $\text{CH}_2\text{Cl}_2$ , the lowest-energy absorption band of TTQA within the range of 500–650 nm shows the maximum ( $\lambda_{\text{abs}}$ ) at 607 nm (Figure 3). The  $\lambda_{\text{abs}}$  of TTQA is largely red-shifted

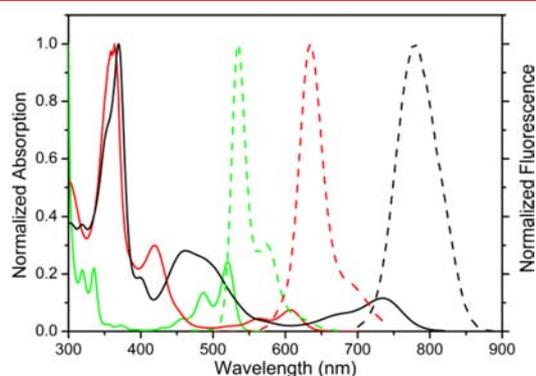


**Figure 3.** UV-vis absorption (solid lines) and fluorescence (dashed lines) spectra of  $\text{C}_8\text{-QA}$  (green), TTQA (red), and DCNTTQA (black) in dilute solution ( $1 \times 10^{-5}$  M in  $\text{CH}_2\text{Cl}_2$ ).

compared with that of  $\text{C}_8\text{-QA}$  ( $\lambda_{\text{abs}} = 522$  nm), reflecting the effect of the fusion of thiophene rings. Replacement of the two carbonyl groups in TTQA with DCN groups further red shifts the  $\lambda_{\text{abs}}$  to the near-infrared (NIR) region ( $\lambda_{\text{abs}} = 735$  nm for DCNTTQA). The optical band gaps of TTQA and DCNTTQA are estimated to be 1.92 and 1.55 eV, respectively, which are close to the energy gaps obtained from the electrochemical data. The variation trend of luminescence spectra is consistent with that of the absorption spectra (Figure 3). TTQA displays deep-red emission ( $\lambda_{\text{em}} = 641$  nm), with a photoluminescence quantum

yield ( $\Phi_{\text{PL}}$ ) of 0.55, which is in sharp contrast to the green emission of  $\text{C}_8\text{-QA}$  ( $\lambda_{\text{em}} = 533 \text{ nm}$ ). Impressively, DCNTTQA shows NIR emission ( $\lambda_{\text{em}} = 748 \text{ nm}$ ,  $\Phi_{\text{PL}} < 0.01$ ).

Due to perfect solubility, solution-processed thin films of DCNTTQA can be prepared and characterized. The lowest-energy absorption band of DCNTTQA film ( $\lambda_{\text{abs}} = 758 \text{ nm}$ ) is red-shifted compared with that of the solution (Figure S3). This implies the existence of intermolecular interactions in the thin film. The aggregation behavior of DCNTTQA was also investigated in solution by concentration-dependent  $^1\text{H}$  NMR. As depicted in Figure 4, all signals for the aromatic protons of

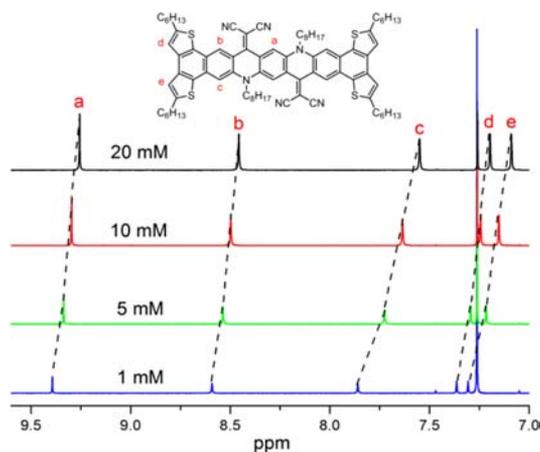


**Figure 4.** Concentration-dependent  $^1\text{H}$  NMR spectra of DCNTTQA in  $\text{CDCl}_3$ .

DCNTTQA show an upfield shift upon increasing concentration from  $1 \times 10^{-3}$  to  $2 \times 10^{-2} \text{ M}$ , which is evidence for the intermolecular  $\pi$ -stacking.<sup>19</sup> A similar phenomenon was observed for *n*-butyl-substituted QA.<sup>15</sup> The above results indicate that the intermolecular  $\pi$ - $\pi$  interactions can exist in thin films and solutions of DCNTTQA in spite of its nonplanar molecule conformation. However, the  $\pi$ -stacking tendency/strength of DCNTTQA should be weaker than that of TTQA as deduced from the solubility comparison.

Taking advantage of the excellent solubility and low-lying HOMO and LUMO energy levels of DCNTTQA, we fabricated solution-processed OFET devices with a bottom-gate, bottom-contact configuration. Gold source and drain electrodes were deposited onto octadecyltrichlorosilane (OTS)-modified  $\text{SiO}_2/\text{Si}$  substrates. The thin film of the active layer was prepared by spin-coating the chloroform solution of DCNTTQA. DCNTTQA exhibits typical p-channel FET characteristics under ambient conditions, which is in contrast to the n-type character of analogous DCN-substituted QA derivatives without substitution and fusion of thiophene rings.<sup>16b</sup> We therefore infer that the reversal of charge transport properties from n-type to p-type is attributed to the fusion of electron-rich thiophene groups that can enhance the hole transport ability.<sup>9</sup> The device without annealing treatment only shows a mobility ( $\mu$ ) of  $6.61 \times 10^{-5} \text{ cm}^2 \text{ V}^{-1} \text{ s}^{-1}$ , while the device annealed at the optimized temperature of  $100 \text{ }^\circ\text{C}$  shows a mobility as high as  $0.217 \text{ cm}^2 \text{ V}^{-1} \text{ s}^{-1}$ , with an on/off current ratio ( $I_{\text{on/off}}$ ) of  $\sim 10^6$  and a threshold voltage of  $-11.0 \text{ V}$  (Figure 5a,b). The X-ray diffraction (XRD) pattern of the pristine film exhibits no diffraction peak, while upon annealing the film at  $100 \text{ }^\circ\text{C}$ , an intense diffraction peak appears at  $5.2^\circ$  (Figure S4). Atomic force microscopy (AFM) images (Figure 5c,d) indicate that the surface of the annealed film

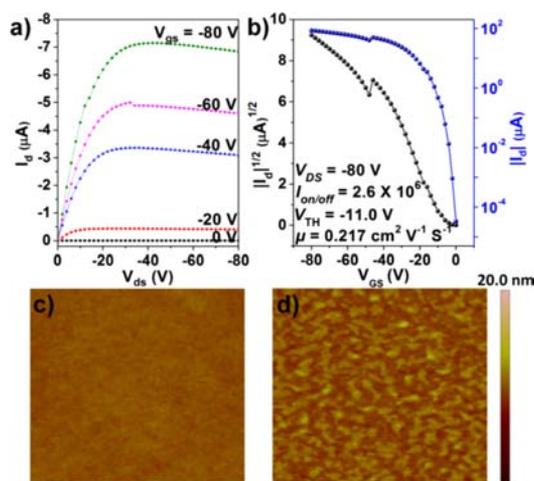


**Figure 5.** Output (a) and transfer (b) characteristics of the OFET device annealed at  $100 \text{ }^\circ\text{C}$  and AFM images ( $5 \times 5 \mu\text{m}$ ) of the pristine (c) and annealed (d) films of DCNTTQA on the OTS-treated  $\text{SiO}_2/\text{Si}$  substrate.

is much rougher than that of the pristine film. The XRD and AFM results reveal that the pristine film is smooth and continuously amorphous, while the annealed film gains certain crystallinity. As a result, the annealed film displays much higher mobility.<sup>20</sup> It is notable that the OFET performance of DCNTTQA is among the best results ever reported on QA-based small molecules and polymers.<sup>21</sup> More importantly, such good performance is achieved through solution processing of small molecules, which avoids the use of high-cost vacuum deposition technology normally adopted by small molecules and minimizes the batch-to-batch variation in performance usually observed for polymers. Our results indicate that constructing solution-processable small molecules with a large  $\pi$ -skeleton is an attractive development direction for QA-based OFET materials.

In summary, two QA-based 11-ring-fused hetero-PAHs, TTQA and DCNTTQA, have been synthesized by facile ferric chloride mediated cyclization and a Knoevenagel reaction. Replacement of the carbonyl moieties in TTQA with strongly electron-withdrawing dicyanoethylene groups endows the resulting DCNTTQA with much lower HOMO and LUMO energy levels, as well as a smaller band gap. It also converts the planar skeleton of TTQA to the nonplanar one of DCNTTQA and therefore significantly improves the solubility. TTQA and DCNTTQA show deep-red and NIR emission, respectively, which are much redder than the emission of the parent  $\text{C}_8\text{-QA}$  molecule. Solution-processed OFETs based on DCNTTQA reach a hole mobility of  $0.217 \text{ cm}^2 \text{ V}^{-1} \text{ s}^{-1}$ .

## ■ ASSOCIATED CONTENT

### Supporting Information

The Supporting Information is available free of charge on the ACS Publications website at DOI: 10.1021/acs.orglett.5b03155.

Experimental details, NMR spectra, additional spectra, and data for thermal, electrochemical, photophysical, and XRD studies (PDF)

## ■ AUTHOR INFORMATION

### Corresponding Authors

\*E-mail: zuolunzhang@jlu.edu.cn.

\*E-mail: yugui@iccas.ac.cn

\*E-mail: yuewang@jlu.edu.cn.

## Notes

The authors declare no competing financial interest.

## ACKNOWLEDGMENTS

This work was supported by the National Natural Science Foundation of China (91333201, 51173065 and 21221063), Program for Chang Jiang Scholars and Innovative Research Team in University (No. IRT101713018), and the Strategic Priority Research Program of the Chinese Academy of Sciences (XDB 12030100).

## REFERENCES

- (1) (a) Tang, C. W.; VanSlyke, S. A. *Appl. Phys. Lett.* **1987**, *51*, 913. (b) Hudson, Z. M.; Wang, Z.; Helander, M. G.; Lu, Z.-H.; Wang, S. *Adv. Mater.* **2012**, *24*, 2922. (c) Entwistle, C. D.; Marder, T. B. *Chem. Mater.* **2004**, *16*, 4574.
- (2) Mishra, A.; Bäuerle, P. *Angew. Chem., Int. Ed.* **2012**, *51*, 2020. (b) Anthony, J. E. *Angew. Chem., Int. Ed.* **2008**, *47*, 452.
- (3) (a) Mei, J.; Diau, Y.; Appleton, A. L.; Fang, L.; Bao, Z. *J. Am. Chem. Soc.* **2013**, *135*, 6724. (b) Wang, C.; Dong, H.; Hu, W.; Liu, Y.; Zhu, D. *Chem. Rev.* **2012**, *112*, 2208. (c) Wen, Y.; Liu, Y. *Adv. Mater.* **2010**, *22*, 1331. (d) Chen, W.; Zhang, J.; Long, G.; Liu, Y.; Zhang, Q. *J. Mater. Chem. C* **2015**, *3*, 8219. (e) Tian, H.; Shi, J.; Yan, D.; Wang, L.; Geng, Y.; Wang, F. *Adv. Mater.* **2006**, *18*, 2149. (f) Ye, Q.; Chi, C. *Chem. Mater.* **2014**, *26*, 4046.
- (4) (a) Kohl, B.; Rominger, F.; Mastalerz, M. *Angew. Chem., Int. Ed.* **2015**, *54*, 6051. (b) Tan, Y.-Z.; Osella, S.; Liu, Y.; Yang, B.; Beljonne, D.; Feng, X.; Müllen, K. *Angew. Chem., Int. Ed.* **2015**, *54*, 2927.
- (5) (a) Wang, C.; Zhang, J.; Long, G.; Aratani, N.; Yamada, H.; Zhao, Y.; Zhang, Q. *Angew. Chem., Int. Ed.* **2015**, *54*, 6292. (b) Li, J.; Zhang, Q. *ACS Appl. Mater. Interfaces* **2015**, DOI: 10.1021/acsami.5b00113.
- (6) (a) Dou, C.; Saito, S.; Matsuo, K.; Hisaki, I.; Yamaguchi, S. *Angew. Chem., Int. Ed.* **2012**, *51*, 12206. (b) Matsuo, K.; Saito, S.; Yamaguchi, S. *J. Am. Chem. Soc.* **2014**, *136*, 12580. (c) Fukazawa, A.; Yamada, H.; Yamaguchi, S. *Angew. Chem., Int. Ed.* **2008**, *47*, 5582.
- (7) (a) Fischer, G. M.; Daltrozzi, E.; Zumbusch, A. *Angew. Chem., Int. Ed.* **2011**, *50*, 1406. (b) Fischer, G. M.; Ehlers, A. P.; Zumbusch, A.; Daltrozzi, E. *Angew. Chem., Int. Ed.* **2007**, *46*, 3750.
- (8) (a) Zhang, C.; Shi, K.; Cai, K.; Xie, J.; Lei, T.; Yan, Q.; Wang, J.-Y.; Pei, J.; Zhao, D. *Chem. Commun.* **2015**, *51*, 7144. (b) Lei, T.; Wang, J.-Y.; Pei, J. *Chem. Mater.* **2014**, *26*, 594. (c) Chang, J.; Ye, Q.; Huang, K.-W.; Zhang, J.; Chen, Z.-K.; Wu, J.; Chi, C. *Org. Lett.* **2012**, *14*, 2964. (d) Song, D.; Zhu, F.; Yu, B.; Huang, L.; Geng, Y.; Yan, D. *Adv. Mater.* **2008**, *20*, 2142.
- (9) (a) Fukutomi, Y.; Nakano, M.; Hu, J.-Y.; Osaka, I.; Takimiya, K. *J. Am. Chem. Soc.* **2013**, *135*, 11445. (b) Zhang, W.; Sun, X.; Xia, P.; Huang, J.; Yu, G.; Wong, M. S.; Liu, Y.; Zhu, D. *Org. Lett.* **2012**, *14*, 4382. (c) Ye, Q.; Chang, J.; Huang, K.-W.; Dai, G.; Zhang, J.; Chen, Z.-K.; Wu, J.; Chi, C. *Org. Lett.* **2012**, *14*, 2786.
- (10) (a) Yang, D.-T.; Radtke, J.; Møllerup, S. K.; Yuan, K.; Wang, X.; Wagner, M.; Wang, S. *Org. Lett.* **2015**, *17*, 2486. (b) Yue, W.; Suraru, S.-L.; Bialas, D.; Müller, M.; Würthner, F. *Angew. Chem., Int. Ed.* **2014**, *53*, 6159.
- (11) (a) Faulkner, E. B.; Schwartz, R. J. *High Performance Pigments*; Wiley-VCH: Weinheim, 2009. (b) Labana, S. S.; Labana, L. L. *Chem. Rev.* **1967**, *67*, 1.
- (12) Dou, C.; Wang, C.; Zhang, H.; Gao, H.; Wang, Y. *Chem. - Eur. J.* **2010**, *16*, 10744.
- (13) (a) Fan, Y.; Song, W.; Yu, D.; Ye, K.; Zhang, J.; Wang, Y. *CrystEngComm* **2009**, *11*, 1716. (b) Wang, C.; Chen, D.; Chen, W.; Chen, S.; Ye, K.; Zhang, H.; Zhang, J.; Wang, Y. *J. Mater. Chem. C* **2013**, *1*, 5548.
- (14) Wang, C.; Chen, S.; Wang, K.; Zhao, S.; Zhang, J.; Wang, Y. *J. Phys. Chem. C* **2012**, *116*, 17796.
- (15) Ye, K.; Wang, J.; Sun, H.; Liu, Y.; Mu, Z.; Li, F.; Jiang, S.; Zhang, J.; Zhang, H.; Wang, Y.; Che, C. *J. Phys. Chem. B* **2005**, *109*, 8008.
- (16) (a) Javed, I.; Zhang, Z.; Peng, T.; Zhou, T.; Zhang, H.; Issa Khan, M.; Liu, Y.; Wang, Y. *Sol. Energy Mater. Sol. Cells* **2011**, *95*, 2670. (b) Zhou, T.; Jia, T.; Kang, B.; Li, F.; Fahlman, M.; Wang, Y. *Adv. Energy Mater.* **2011**, *1*, 431.
- (17) Ye, Q.; Chang, J.; Huang, K.-W.; Chi, C. *Org. Lett.* **2011**, *13*, 5960.
- (18) (a) de Miguel, P.; Bryce, M. R.; Goldenberg, L. M.; Beeby, A.; Khodorkovsky, V.; Shapiro, L.; Niemz, A.; Cuello, A. O.; Rotello, V. J. *Mater. Chem.* **1998**, *8*, 71. (b) Takeda, T.; Sugihara, H.; Suzuki, Y.; Kawamata, J.; Aku-tagawa, T. *J. Org. Chem.* **2014**, *79*, 9669.
- (19) (a) Martin, R. B. *Chem. Rev.* **1996**, *96*, 3043. (b) Shetty, A. S.; Zhang, J.; Moore, J. S. *J. Am. Chem. Soc.* **1996**, *118*, 1019.
- (20) Chen, H.; Guo, L.; Yu, G.; Zhao, Y.; Zhang, J.; Gao, D.; Liu, H.; Liu, Y. *Adv. Mater.* **2012**, *24*, 4618.
- (21) (a) Yanagisawa, H.; Mizuguchi, J.; Aramaki, S.; Sakai, Y. *Jpn. J. Appl. Phys.* **2008**, *47*, 4728. (b) Xu, Z.; Xiang, H.; Roy, V. A. L.; Chui, S. S.; Wang, Y.; Lai, P. T.; Che, C.-M. *Appl. Phys. Lett.* **2009**, *95*, 123305. (c) Glowacki, E. D.; Leonat, L.; Irimia-Vladu, M.; Schwödiauer, R.; Ullah, M.; Sitter, H.; Bauer, S.; Sariciftci, N. S. *Appl. Phys. Lett.* **2012**, *101*, 023305. (d) Osaka, I.; Akita, M.; Koganezawa, T.; Takimiya, K. *Chem. Mater.* **2012**, *24*, 1235. (e) Li, H.; Wang, X.; Liu, F.; Fu, H. *Polym. Chem.* **2015**, *6*, 3283.